



## Original research article

# Modelling herbivore population dynamics in the Amboseli National Park, Kenya: Application of spatial aggregation of variables to derive a master model

Victor N. Mose<sup>a,b,c,\*</sup>, Tri Nguyen-Huu<sup>b,c,d</sup>, Pierre Auger<sup>b,c</sup>, David Western<sup>a</sup>

<sup>a</sup> African Conservation Centre (ACC), 15289-00509 Nairobi, Kenya

<sup>b</sup> UMI 209 UMMISCO, IRD, 32, Av. Henri Varagnat, 93143 Bondy cedex, France

<sup>c</sup> UMI 209, UMMISCO, Université Pierre et Marie Curie, F-75005 Paris, France

<sup>d</sup> IXXI, 7 rue du Vercors, 69007 Lyon, France

## ARTICLE INFO

## Article history:

Received 14 January 2011

Received in revised form 8 February 2012

Accepted 20 February 2012

Available online 21 March 2012

## Keywords:

Large parks

Herbivorous

Competition model

Aggregation of variables

## ABSTRACT

The recent expansion of human activities such as agriculture has continuously threatened to block wildlife migration corridors that connect Amboseli National Park (Kenya) to surrounding ecosystems. We study the impact of blocked corridors on herbivore populations using a spatial mathematical model that describes the movements and population dynamics of selected species (zebra, wildebeest and Grant's gazelle) based on resource availability. Aggregation methods are used to reduce the complexity of the model which uses actual parameters calibrated from long term data collected in the area for over three decades. The model suggests the need to maintain these connections to sustain species diversity. Our results show that blocked migration corridors lead to competitive exclusion where only one species survives. However, a possible mechanism of maintenance of biodiversity in the area could be due to an exchange of animals between the park and surrounding ecosystems, when the oscillations of species densities in the ecosystems are out of phase compared to each other and to those within the park.

© 2012 Elsevier B.V. All rights reserved.

## 1. Introduction

Recent expansion of human activities such as agriculture, has continuously threatened to disconnect Amboseli National Park (Fig. 1) from surrounding ecosystems. Blocking of the migration corridors could have a disastrous impact on the species populations inside the park. In order to understand the ecology of large herbivores in fluctuating environments, there is the need for development of mathematical models that can inform conservation managers of remedial policies and practice for sustaining species diversity. The aim of this work is to contribute to a better understanding of the ecological dynamics of the Amboseli ecosystem using mathematical models: we demonstrate the need to maintain migration corridors that connect to other surrounding ecosystems and predict dynamics of population sizes.

The Amboseli ecosystem is complex, with a large number of species interacting in a landscape that fluctuates with seasons, erratic weather patterns, climatic variability and prolonged droughts. In this work, we present a simple model of the spatial population dynamics of the main herbivorous species in Amboseli (zebra, wildebeest and Grant's gazelle), describing their space and

time changes in population density. Aerial surveys on large mammal censuses are counted on a network consisting of two-dimensional patches (5 km × 5 km) connected by dispersal. In our model, we use this collection of patches to represent the environment.

The complete model, which aims at describing the dynamics of population densities in all the patches, must deal with many coupled variables in a set of ordinary differential equations (ODEs). Ordinarily, it is difficult to obtain analytical results from such a system. However, when some processes occur at different time scales, it is possible to simplify the complete model and to derive a reduced model that governs fewer global variables using aggregation of variables methods. Aggregation of variables is a methodology aimed at reducing the complexity (i.e. the number of variables) of large models (Iwasa et al., 1987). In this paper, we use approximate aggregation methods (Iwasa et al., 1989) and more precisely aggregation techniques based on time scale separation methods (Auger and Roussarie, 1994). We also refer to recent papers (Auger et al., 2008a,b) and to the review paper on spatial aggregation of variables (Auger et al., 2012). The resulting aggregated model can be handled easily and provides analytical results.

This paper is organized as follows. Section 2 presents the ecological background of the problem. Section 3 presents the mathematical formulations of the model. Section 4 describes the parameters in the model. Section 5 is devoted to the reduction of the model using aggregation of variables methods. In Section 6, we

\* Corresponding author at: African Conservation Centre (ACC), 15289-00509 Nairobi, Kenya. Tel.: +254 720323683; fax: +254 02891751.

E-mail address: [vnmose@gmail.com](mailto:vnmose@gmail.com) (V.N. Mose).

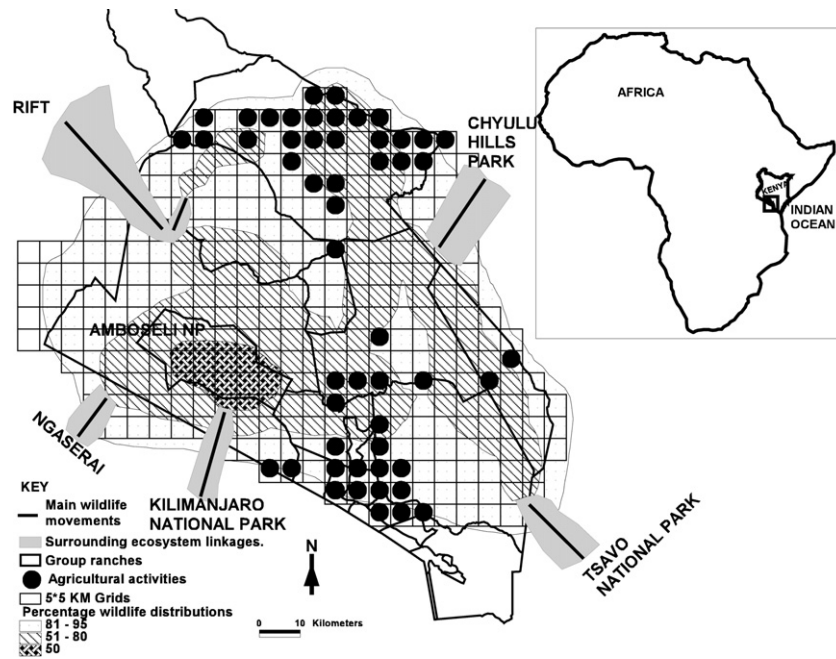


**Fig. 1.** Representation of Amboseli ecosystem in southern Kenya, divided into 5 km × 5 km patches showing possible migration corridors (surrounding ecosystems linkages), wildlife dispersal (percentage wildlife distribution) derived from long term Amboseli data and agriculture expansion in recent times (black dots).

discuss the results and compare the dynamics of the model with and without migration corridors. Section 7 concludes the paper.

## 2. Ecological background

The Amboseli ecosystem covers an area of 8500 km<sup>2</sup> in southern Kenya, close to the Tanzanian border and lies at an altitude of 1200 m. The ecosystem encompasses the region utilized by migratory large ungulates and pastoral livestock that concentrate each dry season around permanent swamps fed by Mt. Kilimanjaro (Western, 1975). The open terrain and regular counts of the populations and spatial distributions of all herbivores weighing greater than 15 kg since 1967 (Western and Nightingale, 2004) make Amboseli an ideal field site for modelling studies.

The aerial surveys on large mammal censuses conducted by the Amboseli Conservation Program (ACP) for over 40 years, are counted on a network consisting of two-dimensional grids (5 km × 5 km) connected by migration. Each patch is classified as one of the eight major types of habitats in Amboseli (dense woodland, open woodland, open bushland, grassland, dense bush, swamp, sveda, swamp edge).

Amboseli National Park lies within the Amboseli ecosystem. Long-term population censuses have shown that wildlife utilize a larger area than the protected national park. On average, 50% of the wildlife is found inside the national Park and 80% in the line shaded area as shown in Fig. 1. This area includes the national park. The Amboseli wildlife populations belong to a larger metapopulation system. The movement of wildlife into and out of the Amboseli ecosystem and the park could be of benefit to the animals in the event of extreme conditions such as drought. In recent years, agricultural activities (black dots in Fig. 1) have rapidly expanded to wildlife dispersal areas threatening to disconnect this ecosystem from the surrounding ones, that also support many different wildlife species. Increasing human settlement and development in the ecosystem will certainly isolate Amboseli National Park. Limiting free movement of wildlife could have severe consequences on long term species survival and species population densities. We propose a mathematical model that describes the population dynamics of the main herbivorous species and test the

effect of isolating the Amboseli ecosystem on the survival of these species.

## 3. Construction of the model

We present a spatially explicit multi-habitat and multi-species resource–consumer model based on a grid system of 5 km × 5 km of the Amboseli ecosystem. The resource considered is grass and the consumer species are primarily grazers. We build a model which includes  $s$  herbivorous species occupying  $A$  patches connected by dispersal. Species forage digestibility differs among species and is governed by the body mass. Individuals within a population select habitats or resources to maximize their forage digestibility and energetic gains (Kshatriya, 1998). The main species we focus on in our analysis are zebra, wildebeest and Grant's gazelle.

We use a demographic model based on energy budget similar to the one developed by Kshatriya (1998). The effect of species body size, digestive constraints of the herbivores and resource abundance are incorporated. For the herbivore population, the net growth rate is equal to the difference between the energy gain from feeding and the energetic cost of maintenance. Individuals of different species redistribute themselves through time in response to changes in population and vegetation densities.

The model is coupled to a dispersal model in which the proportion of animals leaving a patch is driven by the quantity of resource available in that patch. It is also coupled to a migration model, implicitly representing the connection to surrounding parks in southern Kenya.

By using aggregation techniques in a patchy environment and assuming a favourable scenario of a constant amount of grass biomass available for each day, we determine the asymptotic dynamics. Using the model, we explore the importance of maintaining the migration corridors to other ecosystems and investigate long-term species coexistence with and without the connecting corridors.

The model is a combination of two sets of processes: demographic processes which occur at a slow time scale and dispersal processes which occur at a fast time scale. For each

species  $j \in \{1, \dots, s\}$ , its density  $\eta_{ij}$  in patch  $i, i \in \{1, \dots, A\}$ , is governed by

$$\frac{d\eta_{ij}}{dt} = d_{ij}^{demo}(\eta) + d_{ij}^{disp}(\eta) \tag{1}$$

where  $\eta = (\eta_{11}, \dots, \eta_{1s}, \dots, \eta_{A1}, \dots, \eta_{As})$ .  $d_{ij}^{demo}(\eta)$  represents the part of the variation of  $\eta_{ij}$  due to demographic processes and  $d_{ij}^{disp}(\eta)$  represents the part of the variation due to dispersal processes.

The density of grass available depends on the type of habitat in each patch. In patch  $i, i \in \{1, \dots, A\}$ , the density of grass that can be grazed is constant and is denoted as  $K_i$ , so as to simulate favourable scenarios when resources are always available. For each species  $j \in \{1, \dots, s\}$ , the variation of density  $\eta_{ij}$  in patch  $i$  due to demographic processes is given by:

$$d_{ij}^{demo}(\eta) = \frac{\eta_{ij}\beta(e_{ij} - q_j)}{\omega_j} \tag{2}$$

where  $e_{ij}$  is the per capita energy gain of herbivore species  $j$  grazing in patch  $i$ ,  $\omega_j$  is the body mass,  $q_j$  is the active metabolic rate, i.e. the energy spent daily by animals, and  $\beta$  is the conversion factor from energy to biomass.

The per capita energy gain depends on the species characteristics (digestive efficiency, etc.) and on the quantity of food available. Inter specific competition only occurs through the quantity of food made available in each patch for each species. Species occupying the same patch share the food according to factors like the density of individuals for each species and their grazing ability. Thus the per capita energy gain can be expressed in a general way as:

$$e_{ij} = \alpha D_j f_j(\bar{\eta}_i, K_i) \tag{3}$$

where  $D_j$  is the digestive efficiency of species  $j$ ,  $\alpha$  is the energy contained per unit of grass that is assimilated, and  $f_j(\bar{\eta}_i, K_i)$  is the amount of grass grazed per capita and per time unit in patch  $i$  by species  $j$ , which depends on the densities  $\bar{\eta}_i = (\eta_{i1}, \dots, \eta_{is})$  of all species in patch  $i$  and on the grass density in patch  $i, K_i$ . Species share the resources in each patch according to their density and grazing ability.

We introduce the maximum grazing efficiency  $g_j$  which represents the maximum possible intake of grass per unit of time for an individual from species  $j$  (individual species daily food intake cannot exceed the quantity  $g_j$ ). This quantity also represents the ability to compete for food when there are several species: the higher the grazing efficiency, the higher the food intake. In each patch, animals are assumed to be distributed in such way that each species occupy a part of the area which is proportional to its own population number and weighted by its ability to graze  $g_j$ . Populations of species  $j$  access a proportion  $g_j\eta_{ij} / \sum_{j'=1}^s g_{j'}\eta_{ij'}$  of the density of grass  $K_i$  in patch  $i$ .

For one individual from species  $j$ , the quantity of grass available in patch  $i$  is

$$v_{ij} = \frac{1}{\eta_{ij}} \frac{g_j\eta_{ij}}{\sum_{j'=1}^s g_{j'}\eta_{ij'}} K_i = \frac{g_j}{\sum_{j'=1}^s g_{j'}\eta_{ij'}} K_i \tag{4}$$

Individuals from species  $j$  in patch  $i$  graze the available quantity of grass  $v_{ij}$ . However, when grass is abundant, individuals will be limited to the maximum possible intake  $g_j$ . The amount of grass grazed per capita is given by a Holling type II function of the variable  $v_{ij}$

$$f_j(\eta, K_i) = \frac{v_{ij}}{a + \frac{1}{g_j} v_{ij}} \tag{5}$$

$$= \frac{g_j K_i}{a \sum_{j'=1}^s g_{j'} \eta_{ij'} + K_i} \tag{6}$$

The parameter  $a$  is time homogeneous and is set to 1 in order to satisfy the hypothesis that for low quantities of grass, the amount of grass grazed is proportional to  $v_{ij}$ . The growth of the biomass of species  $j$  is then summarized as

$$d_{ij}^{demo}(\eta) = \eta_{ij} \frac{\beta}{\omega_j} \left( \frac{\alpha D_j g_j K_i}{\sum_{j'=1}^s g_{j'} \eta_{ij'} + K_i} - q_j \right) \tag{7}$$

In this model, we use a simple dispersal process: individuals disperse to the neighbouring patches at a rate inversely proportional to the quantity of food available in the patch they are in. Intuitively, individuals are more likely to stay if food is sufficiently available in their current patch. If food is insufficient, they leave the patch. Furthermore, individuals have information on the quantity of food available in their patch, but not on the quantity of food in adjacent patches. Effect of dispersal which is inversely proportional to resources available in a given patch is also considered in El Abdllaoui et al. (2007) and Morozov et al. (2012). We introduce a migration term  $\delta_{ij} - \kappa_{ij}\eta_{ij}$ , where  $\delta_{ij}$  represents a constant input of individuals into the park and  $\kappa_{ij}\eta_{ij}$  an output of animals proportional to the population density.

For each patch  $i$ , let us denote  $V_i$  the set of neighbouring patches. The variation of  $\eta_{ij}$  due to dispersal dynamics for each patch  $i, i \in \{1, \dots, A\}$  and each species  $j, j \in \{1, \dots, s\}$  is given by

$$d_{ij}^{disp}(\eta) = -\frac{1}{\epsilon} \frac{|V_i|}{K_i} \eta_{ij} + \frac{1}{\epsilon} \sum_{i' \in V_i} \frac{1}{K_{i'}} \eta_{i'j} + \delta_{ij} - \kappa_{ij}\eta_{ij} \tag{8}$$

where  $|V_i|$  denotes the number of neighbouring patches. Parameter  $1/\epsilon$  can either be seen as the magnitude or the speed of the dispersal process. The smaller the  $\epsilon$ , the faster the dispersal process.

In order to describe the global dynamics, demographic processes and dispersal processes have to be combined. The set of equations governing the dynamics reads:

$$\frac{d\eta_{ij}}{dt} = \eta_{ij} \frac{\beta}{\omega_j} \left( \frac{\alpha D_j g_j K_i}{\sum_{j'=1}^s g_{j'} \eta_{ij'} + K_i} - q_j \right) - \frac{1}{\epsilon} \left( \frac{|V_i|}{K_i} \eta_{ij} - \sum_{i' \in V_i} \frac{\eta_{i'j}}{K_{i'}} \right) + \delta_{ij} - \kappa_{ij}\eta_{ij} \tag{9}$$

When migration corridors are blocked,  $\forall i \in \{1, \dots, A\}$  and  $\forall j \in \{1, \dots, s\}$ ,  $\delta_{ij} = 0$  and  $\kappa_{ij} = 0$ .

#### 4. Parameters of the model

The parameter values used in this model were assigned from published sources and from the long term data on vegetation and animals monitored by Amboseli Conservation Program (ACP). The values for grass densities  $K_i$  [kg/km<sup>2</sup>] were determined by calculating the average vegetation available during the year 2008. These values range from  $K = 867$  kg/km<sup>2</sup> for open bushland habitat to  $K = 8556$  kg/km<sup>2</sup> for the swamp habitat.

The digestive efficiency,  $D$  of the herbivore species used in the model (Table 1) were based on Kshatriya (1998) and the digestive kinematics model developed by Illius and Gordon (1992). Similar studies by Ludwig et al. (2008) found that for instance, the maximum intake for wildebeest is about 3700 g per day, close to the ACP calibrations of 3580 g (dry weight) per day for a similar period. The

**Table 1**  
Average body weights, maximum resource intakes, digestive efficiency and metabolic rate parameters used in the model for each species.

| Species         | w [kg] | g [kg/day] | D     | q [MJ/day] |
|-----------------|--------|------------|-------|------------|
| Zebra           | 200    | 4.68       | 0.561 | 19.28      |
| Wildebeest      | 123    | 3.58       | 0.648 | 17.07      |
| Grant's gazelle | 40     | 0.62       | 0.645 | 3.253      |

Source: Amboseli Conservation Program (ACP).

active metabolic rate,  $q_j$  [MJ/day] was based on Murray (1995). Murray (1995) calculated that the wildebeest (143 kg) needs an energy intake of 22.32 MJ/day for maintenance (Ludwig et al., 2008). These parameters were assumed to be constant. The conversion factor from energy to body mass,  $\beta$  [kg/MJ] was set to 0.0365 (Kshatriya, 1998). In the model, the value of parameter  $\alpha$  is the product of energy content ( $ec = 15.6$  MJ/kg), the efficiency of conversion of food energy (ingested energy) into metabolic energy ( $mc = 0.75$ ) (Blaxter, 1980), and fraction of day foraging ( $pd = 17/24$ ) (Kshatriya, 1998). Foraging time is a large component of the daily activity budget of an animal (Fancy and White, 1985). The value of  $\alpha = ec \times mc \times pd$  was therefore set to ( $\alpha = 8.288$ ) in this model.

The initial density distribution values used in the model were actual aerial survey estimates for the year 2008. The quantity  $\epsilon K_i / |V_i|$  represents the average time spent by an animal in patch  $i$ . From field observation, parameter  $\epsilon$  has been roughly estimated to be  $\leq 0.1$ , which corresponds to an average time of 10–100 days (depending on the resource considered) or lesser. Analysis was performed for  $\epsilon = 0.1$ ; results are still valid for smaller values. Other simulations were performed for  $\epsilon = 5$  to show that the qualitative results are robust even when dispersal processes are not considered to occur at a fast time scale.

Migration to and from other parks has not been estimated from real data: in this paper, we study the effect of migration corridors on coexistence of species inside the Amboseli ecosystem. We compare a scenario where a small input and output (200 animals for each species entering the entire area and 1% leaving the area each day) to a scenario without the migration corridors. These values are small enough to consider that the process occurs at slow time scale.

### 5. Aggregated model

The complete model governs  $A \times s = 1500$  variables and consists of the same number of differential equations. Even if it is possible to simulate the dynamics of this model, it is hard to give analytical results and the mathematical predictions of the model dynamics. We now build an approximate model which consists of  $s = 3$  equations governing the total species densities (i.e. total densities obtained by summation of local densities over all patches of the complete spatial domain). This model, called the aggregated model, is mathematically tractable as it is possible to analytically compute its equilibria. The dynamics of the aggregated model is an approximation of the original global model.

When dispersal is fast in comparison with demographic processes, it is possible to build an approximate simplified model using reductions methods called aggregation of variables based on perturbation techniques and on the application of a center manifold theorem of Fenichel (Auger and Poggiale, 1995). The model is reduced to an aggregated model that consists of a system of fewer equations by using difference between timescales (see Appendix A for a more detailed explanation).

When  $\epsilon$  is small, demographic processes occur at a much slower time scale than dispersal processes. We can introduce a fast time scale by considering,  $\tau = t/\epsilon$  which can be related to the dispersal processes. When describing the dynamics at fast time scale, Eq. (9) now reads:

$$\frac{d\eta_{ij}}{d\tau} = \epsilon \eta_{ij} \frac{\beta}{\omega_j} \left( \frac{\alpha D_j g_j K_i}{\sum_{j=1}^s g_j \eta_{ij} + K_i} - q_j \right) - \frac{|V_i|}{K_i} \eta_{ij} + \sum_{i' \in V_i} \frac{\eta_{i'j}}{K_{i'}} + \epsilon (\delta_{ij} - \kappa_{ij} \eta_{ij}) \quad (10)$$

We first assume that  $\epsilon = 0$  in Eq. (10) and determine if there is a stable equilibrium. Such an equilibrium is achieved when individuals are distributed proportionally to the available

resources in each patch. Thus density of animals  $\eta_{ij}$  of species  $j$  in patch  $i$  can be inferred from the total density of animals of species  $j$ ,  $\eta_j$  by the following relation (see Appendix A.1):

$$\eta_{ij} = \frac{K_i}{\sum_{i=1}^A K_i} \eta_j \quad (11)$$

This is a stable equilibrium for the fast dynamics. Individuals are distributed according to the Ideal Free Distribution. We then consider  $\epsilon \neq 0$  and assume that in the global model given by Eq. (9), equilibrium is always reached. For each species  $j$ , we determine an equation that governs total population  $\eta_j$  by summing the equations for all patches  $i$

$$\frac{d\eta_j}{dt} = \sum_i \frac{d\eta_{ij}}{dt} \quad (12)$$

We now substitute  $\eta_{ij}$  in Eq. (9) by the value determined in (11) at fast equilibrium. When the expression corresponding to dispersal is null in Eq. (9), Eq. (12) reads:

$$\frac{d\eta_j}{dt} = \eta_j \frac{\beta}{\omega_j} \left( \alpha D_j g_j \frac{G}{\sigma(\eta) + G} - q_j \right) + \delta_j - \kappa_j \eta_j \quad (13)$$

where  $G = \sum_{i=1}^A K_i$  denotes the total quantity of grass,  $\sigma(\eta) = \sum_{j=1}^s g_j \eta_j$ ,  $\delta_j = \sum_{i=1}^A \delta_{ij}$  and  $\kappa_j = \sum_{i=1}^A \kappa_{ij} K_i / \sum_{i=1}^A K_i$ . The way of obtaining this equation is detailed in Appendix A.2. We have now obtained a set of  $s$  differential equations, compared to a system of  $s \times A$  equations for the complete model.

### 6. Results

We now describe the equilibria and their stability for the aggregated model with and without migration corridors. The mathematical results obtained here hold under two conditions that are ecologically relevant:

- viability of all species: we only consider species that are able to survive in conditions when there is no competition. This means that when food is abundant, the energy gained from grazing is greater than energy spent for maintenance. The condition reads:  $\forall j \in \{1, \dots, s\}, \alpha D_j g_j > q_j$  (14)
- species have different parameters: we have determined the following equilibria under the condition that ratios  $\alpha D_j g_j / q_j$  are different for each  $j \in \{1, \dots, s\}$ . If it was not the case, other equilibria could exist, but the fact that two ratios would exactly be the same does not make sense ecologically.

The equilibria are determined from Eqs. (13) and their stability is tested by the analysis of the eigenvalues of the Jacobian matrix.

#### 6.1. Analytical results for the aggregated model: case without corridors

The system has the following equilibria:

- the origin (0, 0) is an unstable equilibrium;
- there are  $s$  non-trivial equilibria  $E_j^* = (0, \dots, 0, \eta_j^*, 0, \dots, 0), j \in \{1, \dots, s\}$ , where  $\eta_j^* = \left( \frac{\alpha D_j}{q_j} - \frac{1}{g_j} \right) G$  (15)

Let us consider  $j_0 \in \{1, \dots, s\}$  such that for all  $j \in \{1, \dots, s\}, j \neq j_0, g_j \eta_j^* < g_{j_0} \eta_{j_0}^*$ . Then  $E_{j_0}^*$  is a stable equilibrium, while for  $j \neq j_0, E_j^*$  are saddle points.

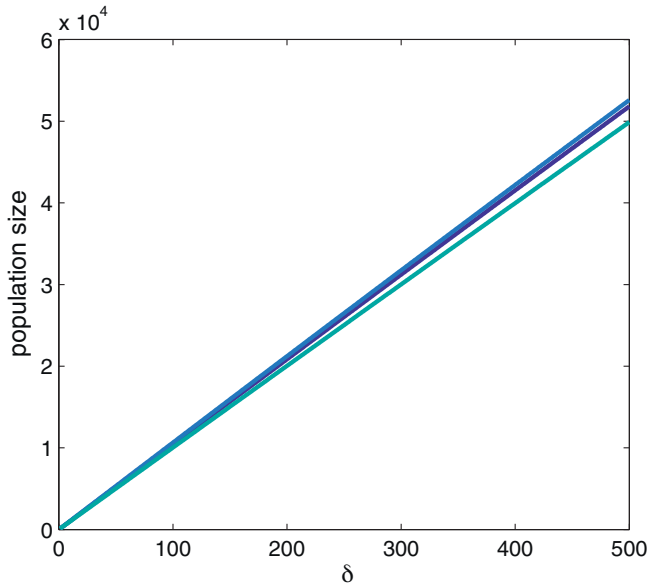


**Fig. 2.** Species densities at equilibrium for different values of  $\delta$  (parameters  $\delta_{ij}$  are the same for every species and are equal to  $\delta$ ).

To summarize, the system presents one non-trivial stable equilibrium and  $s - 1$  non-trivial saddle point. The origin is always an unstable equilibrium (see details in Appendix B). There is no equilibrium for which several species can coexist. This can be interpreted as competitive exclusion: only the most competitive species can survive. This corresponds to the one which has the best grazing ability, i.e. the one that maximizes  $(\alpha D_j g_j / q_j - 1)$ .

**6.2. Analytical results for the aggregated model: case with corridors**

There exists a unique non-negative equilibrium  $\eta^*$ , which is a stable equilibrium (see Appendix C). In the case without corridors, we determined that asymptotically only the zebra survive. In the present case, adding a narrow migration corridor to the previous model introduces a stable equilibrium, which guarantees

coexistence even if the animal densities are very low. The equilibrium always exists when parameters  $\delta_{ij}$  are positive. The values at equilibrium depend on parameters  $\delta_{ij}$  and  $\kappa_{ij}$ . When these parameters tend toward zero, densities at equilibrium also tend toward zero. The dependence on  $\delta_{ij}$  of densities at equilibria are shown in Fig. 2. When there are no migration corridors, the equilibrium 0 is unstable. However, with migration corridors present, the equilibrium of the model is always stable and is close to 0 for a very small  $\delta$ .

**6.3. Numerical results**

Simulations for the model with implicitly represented corridors (Fig. 3) and without corridors (Fig. 4) illustrate that the aggregated model provides reliable results to approximate the dynamics of the complete model. In these figures, dynamics of the complete model are represented by solid lines while those of the aggregated model are represented by dotted lines. Equilibria given by aggregated model are qualitatively the same. The closer  $\epsilon$  is to 0, the closer the values obtained from the complete model to those obtained from the aggregated model. Dynamics are shown for  $\epsilon = 0.1$  (Figs. 3(a) and 4(a)). The dynamics of the complete and aggregated model are very close. We illustrate the robustness of aggregation methods by showing dynamics for very high values of  $\epsilon$  on Figs. 3(b) and 4(b) ( $\epsilon = 5$ ). The dynamics are still qualitatively the same. The difference of the value at equilibrium is more important (Fig. 3(b)) and the time to reach equilibrium is longer (Fig. 4(b)). Fig. 5 illustrates that spatial distribution tends toward the one predicted by the aggregated model. The curves correspond to the sums of population densities in the patches of the same habitat (woodland, bushland, etc.) and not the densities in each patch.

For the first case (blocked migration corridors), the analytical results given by the aggregated model allow us to make predictions about the dynamics of the complete model: the results allow us to determine the equilibria and whether or not the dynamics tend toward these equilibria. Possible equilibria values for each species are presented in Table 2. For each species, the equilibrium value correspond to the number of individuals that can be reached after a transient period in the Amboseli area, when other species have disappeared. The table also represents the corresponding densities.

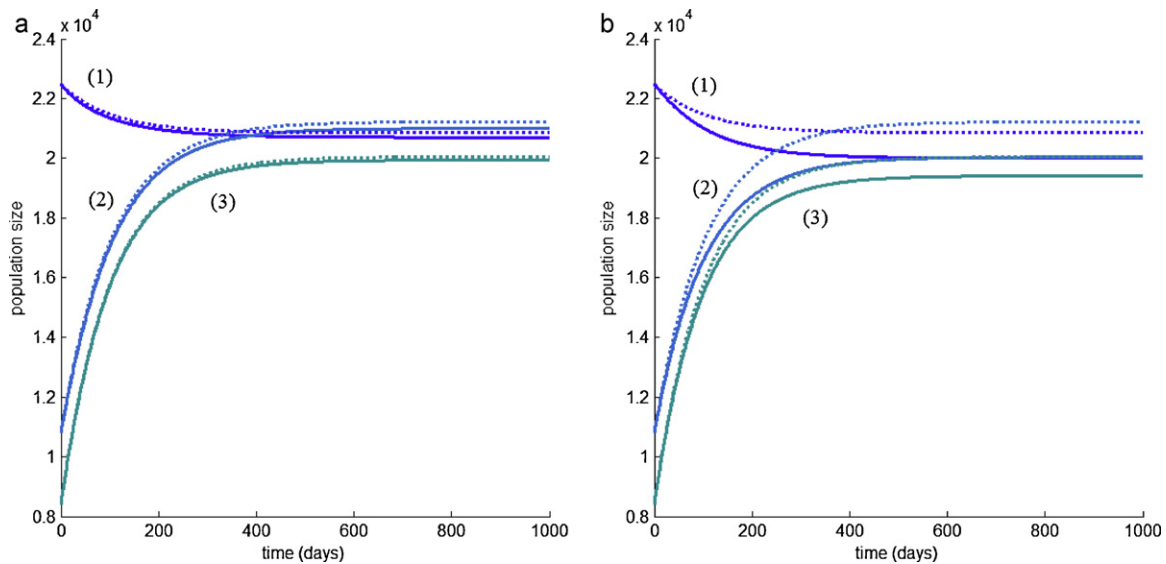


**Fig. 3.** Model output with migration corridors to other parks for  $\epsilon = 0.1$  (a) and  $\epsilon = 5$  (b). Time series are shown for total population density for zebra (1), wildebeest (2) and Grant's gazelle (3) for  $\delta_{ij} = 200/A$  and  $\kappa_{ij} = 0.01$ . Parameters are presented in Section 4. The complete model corresponds to the solid lines, and the aggregated model to the dotted line. All species survive in the long term. Aggregated model and complete model give qualitatively similar outputs. The values at equilibrium for the complete model are closer to the ones of the aggregated model when  $\epsilon$  is small.

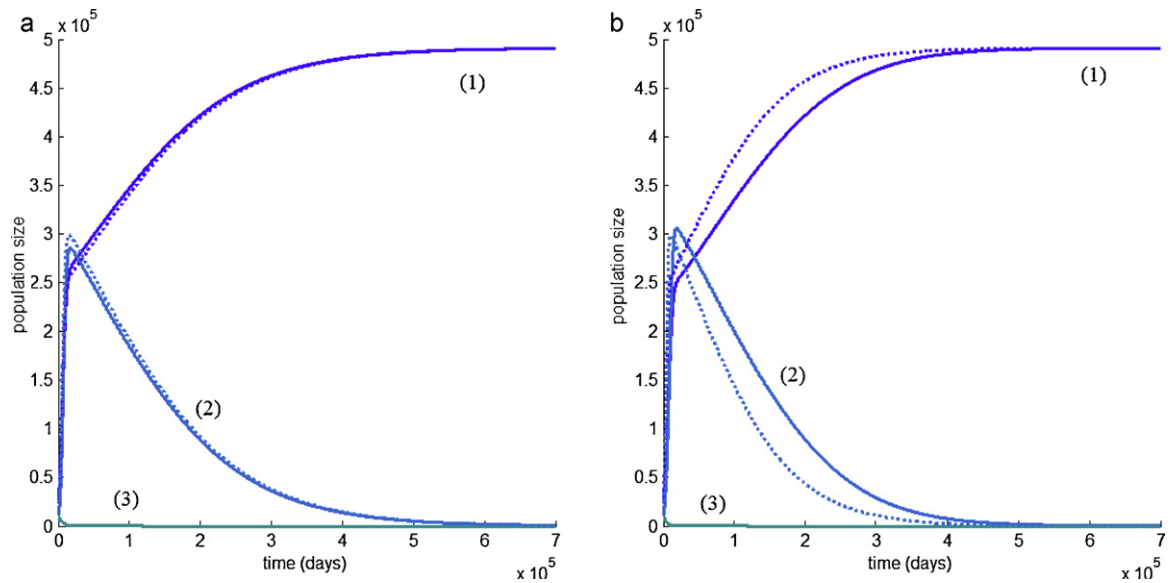


**Fig. 4.** Model output for the blocked migration corridors case for  $\epsilon = 0.1$  (a) and  $\epsilon = 5$  (b). Time series for total population density for zebra (1), wildebeest (2) and Grant's gazelle (3). Parameter are presented in Section 4. Output for the complete model is represented by a solid line, and output for aggregated model by the dotted line. Wildebeest and Grant's gazelle become extinct. For  $\epsilon = 0.1$ , the complete model converges toward the equilibrium faster than for greater values of  $\epsilon$  (here a high value for  $\epsilon$  has been chosen to emphasize the difference between the dynamics).

The values  $g_i \eta_j^*$  allow us to predict which species will survive asymptotically: according to the previous mathematical results, the species with the highest value survives. Others go extinct.

According to results shown in Table 2, we determine that only zebra survives, reaching a total population of around 492,000 individuals in Amboseli, translating to approximately 40 individuals per square kilometre.

Time series of population densities is shown on Fig. 4(a) for  $\epsilon = 0.1$  for both complete and aggregated model. After some transient dynamics, both zebra and wildebeest populations seem

to increase while Grant's gazelle population goes extinct, wildebeest population eventually drops while zebra population reaches its equilibrium. With the parameters determined from Amboseli data, the disappearance of Grant's gazelle is at the scale of a century (decrease of 95% after 46 years for the aggregated model, 49 years for the complete model) while extinction of wildebeests occurs after a much longer time (peak population for wildebeest occurs during year 45 for the aggregated model and year 57 for the complete model).

The peak for wildebeest population is reached during year 70 and Grant's gazelle population drops to under 5% of initial population after 89 years. According to these results, the aggregated model proves efficient in determining the asymptotic dynamics, giving good analytical results with a reduced system of equations. The difference from the complete model lies in the delay in reaching equilibrium.

Fig. 5 shows the distribution of one species (zebra) among the different habitats when the migration corridors are blocked. The shown distribution depends on the availability of resource in different patches within the different major habitats in the Amboseli area. After some transient dynamics, distribution tends toward Ideal Free Distribution among the habitat, maximizing the amount of grass that can be grazed per capita. For the aggregated model, this distribution is always achieved because it corresponds to the fast equilibrium (equilibrium for the dispersal model). Fig. 4 illustrates the difference between the complete model and the aggregated model. For the aggregated model individuals are always distributed according to an Ideal Free Distribution. For

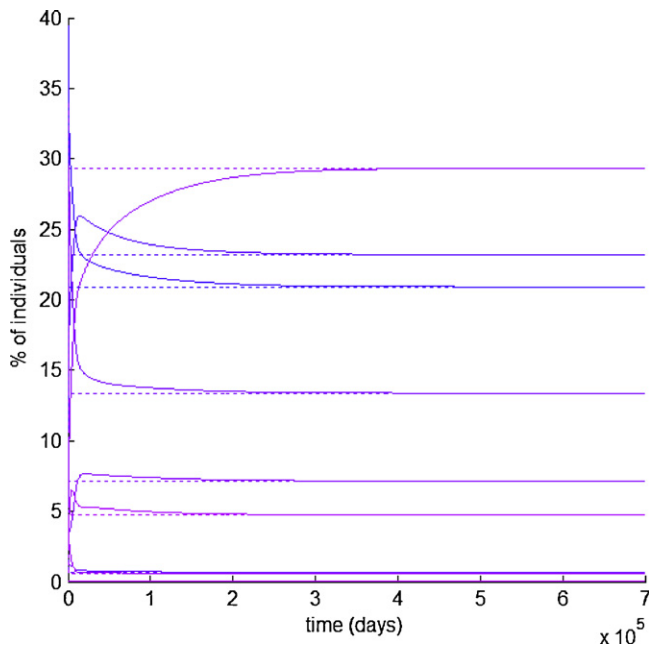


**Fig. 5.** Zebra distribution across different habitats (top to bottom: dense woodland, open woodland, open bushland, grassland, dense bush, swamp, sueda, swamp edge, area surroundings) for  $\epsilon = 0.1$  and case without migration corridors. The other parameters are described in Section 4. Output for the complete model is represented by a solid line and output for aggregated model by the dotted line. Both dynamics tend toward the same distribution.

**Table 2**

Total population and density values for each species at their respective equilibria. The variable shown in the last column allows us to predict the long-term survival of species. The species with the highest value of this variable survives, the others become extinct in the area.

| Species         | Population at equilibrium [individuals] | Density [ind/km <sup>2</sup> ] | $\frac{\alpha D_i \beta_j}{q_j} - 1$ |
|-----------------|---|--------------------------------|--------------------------------------|
| Zebra           | 491,112                                 | 39.3                           | 0.1275                               |
| Wildebeest      | 603,560                                 | 50.5                           | 0.1253                               |
| Grant's gazelle | 519,777                                 | 41.6                           | 0.01788                              |

the complete model, the distribution slowly tends toward the Ideal Free Distribution. The speed of the convergence depends on the scale difference (i.e.  $\epsilon$ ) between dispersal and demography. The faster the dispersal, the faster the Ideal Free Distribution is achieved.

For the second case (open migration corridors), the analytical results obtained with the aggregated model predicts the coexistence of zebra, wildebeest and Grant's gazelle. Although there are many other factors that influence species density distribution and are not considered in this model, the findings have potentially important implications for the functionality of the Amboseli ecosystem. The numerical simulations of the model show that the three animal species can coexist for  $\epsilon = 0.1$  (Fig. 3(a)). For a small constant input of 200 individuals per day in the total area for each species, and a daily output of 1%, at the equilibrium of the aggregated model we have 20,851 zebras, 21,223 wildebeests and 20,045 Grant's gazelles. The equilibrium for the complete model has slightly different values.

## 7. Conclusion

Although Amboseli ecosystem has shown signs of resilience over time, there are reasons to believe that the massive herbivore population declines during the 2009 drought would not have begun recovery, had it not been for the linkages to Tsavo National Park and Tanzania. Our model show the need to allow free flow of wildlife populations into and out of the ecosystem. When the connections are blocked, our model predicts competitive exclusion where only one species survives. However, with open connections, the model predicts species coexistence. We suggest that the surrounding ecosystems show species population dynamics which are out of phase compared to those in the Amboseli area. It is possible to maintain an exchange of animals between the ecosystems which is not synchronized with patterns of animal dispersal within the park, and hence maintain biodiversity in Amboseli area. When there is a large number of surrounding ecosystems with unsynchronized oscillations of densities, the total influx  $\delta_j$  is approximately constant and is equal to its mean value.

The model suggests that a disconnected Amboseli ecosystem will certainly not be able to support the many wildlife species that exist in it. In Amboseli, the uncontrolled expansion of agriculture and human settlement risks blocking of possible migration corridors that could lead to a scenario similar to our model predictions in the case of blocked migration corridors. By carefully mapping out these corridors for wildlife utilization, situations that may lead to competitive exclusion could be avoided. For proper functionality of the already stressed Amboseli ecosystem due to general loss of biodiversity, frequent droughts and possible climate change, there is an urgent need to control human activities around the park. Our model can certainly help in guiding conservation policy formulation.

We assumed for simplicity that the grass available each day for grazing was constant in each habitat and patch of the spatial network. This allowed us to derive from the complete model, a reduced model governing the total densities of animals at a slow time scale. This aggregated model was helpful since we could obtain analytical results about the asymptotic behavior of the system. Looking ahead, it is also possible to suppress corridors selectively, since different species may respond differently to increased human activities.

## Acknowledgements

We would like to thank the international doctoral program PDI MSC of the University of Paris VI for financial support, the Institute

of Research and Development (IRD) in East Africa for local coordination efforts and the African Conservation Centre (ACC), Amboseli Program for providing the data.

## Appendix A. Construction of the aggregated model

When  $\epsilon$  is small, dispersal is fast compared to demography. We introduce a fast time scale by considering  $\tau = t/\epsilon$  and rewrite Eq. (9)

$$\frac{d\eta_{ij}}{d\tau} = \epsilon \eta_{ij} \frac{\beta}{\omega_j} \left( \frac{\alpha D_j g_j K_i}{\sum_{j'=1}^s g_{j'} \eta_{ij'} + K_i} - q_j \right) - \frac{|V_i|}{K_i} \eta_{ij} + \sum_{i' \in V_i} \frac{\eta_{i'j}}{K_{i'}} + \epsilon (\delta_{ij} + \kappa_{ij} \eta_{ij}) \quad (\text{A.1})$$

We now consider the model as an  $\epsilon$ -perturbation of the non-perturbed problem obtained for  $\epsilon = 0$  in Eq. (A.1). Thus we first consider the dispersal part of the dynamics in Eq. (A.1).

### A.1. Analysis of fast dynamics

The analysis of dispersal dynamics is a very classic problem. Analysis of this stochastic process shows that the system tends toward a stable equilibrium, that we call fast equilibrium. The equilibrium is obtained for values of  $\eta_{ij}$  that verify for every  $i$  and  $j$

$$-\frac{|V_i|}{K_i} \eta_{ij} + \sum_{i' \in V_i} \frac{1}{K_{i'}} \eta_{i'j} = 0 \quad (\text{A.2})$$

This equilibrium is reached when animal densities are distributed among patches proportionally to the availability of resources, thus realizing the Ideal Free Distribution. At fast equilibrium, for species  $j$ , the density of animals in patch  $i$  is then proportional to the quantity of grass available every day in that patch. Density  $\eta_{ij}$  of species  $j$  in patch  $i$  can be inferred from the total density of species  $j$ ,  $\eta_j$  by the following relation:

$$\eta_{ij} = \frac{K_i}{\sum_{i'=1}^A K_{i'}} \eta_j \quad (\text{A.3})$$

We denote  $G = \sum_i K_i$  the total quantity of grass. This equilibrium is hyperbolically stable for the fast system, which means that this set of fast equilibria constitutes an attracting invariant set for small positive values of  $\epsilon$ .

### A.2. Aggregated model

We build an approximate model using aggregation methods based on Fenichel theorem (Auger and Poggiale, 1995). Aggregation methods are detailed in the present issue, see also Carr (1981), Fenichel (1971), Hirsch et al. (1970).

In order to build the aggregated model, we substitute  $\eta_{ij}$  in Eq. (9) with the value determined in (A.3) at fast equilibrium. In every equation of the system, the expression corresponding to dispersal is null according to Eq. (A.2). Let us describe the system at slow time scale. Eq. (9) now reads:

$$\frac{d\eta_{ij}}{dt} = \eta_{ij} \frac{\beta}{\omega_j} \left( \alpha D_j g_j \frac{K_i}{\sum_{j'=1}^s g_{j'} \eta_{ij'} + K_i} - q_j \right) + \delta_{ij} - \kappa_{ij} \eta_{ij} \quad (\text{A.4})$$

For each species  $j$ , we can obtain a general equation that governs the total density by summing Eq. (A.4):

$$\frac{d\eta_j}{dt} = \sum_i \frac{d\eta_{ij}}{dt} \tag{A.5}$$

$$= \sum_i \left( \eta_{ij} \frac{\beta}{\omega_j} \left( \frac{\alpha D_j g_j K_i}{\sum_{j'=1}^s g_{j'} \eta_{ij'} + K_i} - q_j \right) + \delta_{ij} - \kappa_{ij} \eta_{ij} \right) \tag{A.6}$$

$$= \sum_i \frac{K_i}{G} \eta_j \frac{\beta}{\omega_j} \left( \frac{\alpha D_j g_j K_i}{\sum_{j'=1}^s g_{j'} \frac{K_i}{G} \eta_{j'} + K_i} - q_j \right) + \delta_j - \kappa_j \eta_j \tag{A.7}$$

$$= \eta_j \frac{\beta}{\omega_j} \sum_i \frac{K_i}{G} \left( \frac{\alpha D_j g_j G}{\sum_{j'=1}^s g_{j'} \eta_{j'} + G} - q_j \right) + \delta_j - \kappa_j \eta_j \tag{A.8}$$

where  $\delta_j = \sum_{i=1}^A \delta_{ij}$  and  $\kappa_j = \sum_{i=1}^A \kappa_{ij} K_i / \sum_{i=1}^A K_i$ . This leads to the following set of equations:

$$\frac{d\eta_j}{dt} = \eta_j \frac{\beta}{\omega_j} \left( \frac{\alpha D_j g_j G}{\sigma(\eta) + G} - q_j \right) + \delta_j - \kappa_j \eta_j \tag{A.9}$$

where  $\sigma(\eta) = \sum_{j'=1}^s g_{j'} \eta_{j'}$ .

### Appendix B. Analysis of the aggregated model without migration corridors

In this appendix, we detail the calculation of equilibria and their stability. When there is no migration corridors,  $\delta_{ij} = 0$  and  $\kappa_j = 0$ . Before determining the equilibria, we compute the Jacobian matrix  $J$  associated with the system in the general case at an arbitrary point as the result is used for different cases when determining stability.

$$J_{j,k} = \frac{\partial h_j}{\partial \eta_k} \tag{B.1}$$

where  $h_j$  corresponds to right term of Eq. (13) such that for all  $j \in \{1, \dots, s\}$ ,  $\frac{d\eta_j}{dt} = h_j(\eta_1, \dots, \eta_s)$ . We now determine the elements of the Jacobian: for all  $j \in \{1, \dots, s\}$ , we have

$$J_{j,j} = \frac{\partial h_j}{\partial \eta_j} \tag{B.2}$$

$$= \frac{\beta}{\omega_j} \left( \alpha D_j g_j G \frac{\sigma(\eta) + G - \eta_j g_j}{(\sigma(\eta) + G)^2} - q_j \right) \tag{B.3}$$

and for  $j \neq k$ ,

$$J_{j,k} = \frac{\partial h_j}{\partial \eta_k} \tag{B.4}$$

$$= -\eta_j \frac{\beta \alpha D_j g_j}{\omega_j} \frac{G g_k}{(\sigma(\eta) + G)^2} \tag{B.5}$$

We now determine the equilibria of the aggregated model. Those equilibria correspond to the sets of values for  $\eta_j$  that verify

$$\forall j \in \{1, \dots, s\}, \frac{d\eta_j}{dt} = 0.$$

**Trivial equilibria:** the point 0 is a trivial equilibrium. We determine the elements of the Jacobian  $J(0)$  at origin from (B.3): for  $j \in \{1, \dots, s\}$ ,

$$J_{j,j}(0) = \frac{\beta}{\omega_j} (\alpha D_j g_j - q_j) \tag{B.6}$$

and from (B.5), we obtain for  $k \neq j$ ,  $J_{j,k}(0) = 0$ . The equilibrium is unstable if and only if there exists  $j \in \{1, \dots, s\}$  such that  $\alpha D_j g_j > q_j$ . This condition can be easily interpreted: in order for a species  $j$  to survive, energy gained from grazing must be greater than the active metabolic energy  $q_j$  when there is no competition for resources. If this condition is not fulfilled always, it leads to extinction of species  $j$ , and there is no interest in the asymptotic dynamics of species  $j$ . We assume from now that this condition is verified for all  $j \in \{1, \dots, s\}$ , i.e.

$$\forall j \in \{1, \dots, s\}, \alpha D_j g_j > q_j \tag{B.7}$$

**Non-trivial equilibria:** we try to determine a non-trivial equilibrium  $(\eta_1^*, \dots, \eta_s^*)$ . This equilibrium verifies for all  $j$

$$\eta_j^* = 0 \quad \text{or} \quad \alpha D_j g_j \frac{G}{\sigma(\eta^*) + G} = q_j.$$

The second equation is equivalent to

$$\sigma(\eta^*) + G = \frac{\alpha D_j g_j G}{q_j} \tag{B.8}$$

In the second equation, the left term does not depend on  $j$ . So there exists a constant  $\zeta \in \mathbb{R}$ , for all  $j \in \{1, \dots, s\}$  such that  $\eta_j^* \neq 0$ ,  $(\alpha D_j g_j) / q_j = \zeta$ .

Ecologically speaking, it is irrelevant the equation  $(\alpha D_j g_j) / q_j = (\alpha D_{j'} g_{j'}) / q_{j'}$  is verified for two different species  $j$  and  $j' \neq j$ . We therefore discard such cases from our study. We then consider  $s$  non-trivial equilibria  $E_j^*, j \in \{1, \dots, s\}$  such that  $E_j^* = (0, \dots, 0, \eta_j^*, 0, \dots, 0)$ . From Eq. (B.8), we determine that  $\eta_j^*$  verifies

$$\eta_j^* = \left( \frac{\alpha D_j}{q_j} - \frac{1}{g_j} \right) G \tag{B.9}$$

We now determine stability for  $E_j^*$ . Reindexing the equations does not modify the dynamics of the system, thus we only have to determine stability for  $E_1^*$  by considering the Jacobian  $J^*$  at this equilibrium. From Eq. (B.5), we deduce that for  $j, k \in \{1, \dots, s\}$  with  $j \neq 1$  and  $j \neq k$ ,  $J_{j,k}^* = 0$ . The Jacobian is then a triangular matrix, and its eigenvalues are given by diagonal coefficients. We now determine these eigenvalues:

$$J_{1,1} = \frac{\beta}{\omega_1} \left( \alpha D_1 g_1 G \frac{G}{(g_1 \eta_1^* + G)^2} - q_1 \right) \tag{B.10}$$

$$= \frac{\beta}{\omega_1} \left( \frac{\alpha D_1 g_1 G^2}{((\alpha D_1 g_1 / q_1) G - G + G)^2} - q_1 \right) \tag{B.11}$$

$$= \frac{\beta}{\omega_1} \left( \frac{q_1^2}{\alpha D_1 g_1} - q_1 \right) \tag{B.12}$$

$$= \frac{\beta q_1}{\omega_1} \left( \frac{q_1}{\alpha D_1 g_1} - 1 \right) \tag{B.13}$$

We then deduce from condition (B.7) that  $J_{1,1} < 0$ .

We now determine the other elements of the diagonal: for all  $k \in \{2, \dots, s\}$  we have:

$$J_{k,k} = \frac{\beta}{\omega_k} \left( \alpha D_k g_k \frac{G}{g_1 \eta_1^* + G} - q_k \right) \quad (\text{B.14})$$

$$= \frac{\beta q_k}{\omega_k} \left( \frac{\alpha D_k g_k G}{q_k} \frac{1}{g_1 \eta_1^* - g_k \eta_k^* + ((\alpha D_k g_k G)/q_k)} - 1 \right) \quad (\text{B.15})$$

We deduce that  $J_{k,k} < 0$  if and only if  $\alpha D_k g_k G/q_k < g_1 \eta_1^* - g_k \eta_k^* + \alpha D_k g_k G/q_k$ , and so  $J_{k,k} < 0$  if and only if  $g_k \eta_k^* < g_1 \eta_1^*$ .

We can now draw conclusions about the stability of equilibrium  $E_1^*$ . Two cases can occur: if for all  $k \in \{2, \dots, s\}$ ,  $g_k \eta_k^* < g_1 \eta_1^*$ , then  $E_1^*$  is stable. If there exists  $k \in \{2, \dots, s\}$  such that  $g_k \eta_k^* > g_1 \eta_1^*$ , then  $E_1^*$  is a saddle point (we discard cases of equality because they are ecologically unlikely to happen).

In summary, the system presents,  $s$  non-trivial equilibria  $E_j^*$ ,  $j \in \{1, \dots, s\}$ . Let us consider  $j_0 \in \{1, \dots, s\}$  such that for all  $j \in \{1, \dots, s\}$ ,  $j \neq j_0$ ,  $g_j \eta_j^* < g_{j_0} \eta_{j_0}^*$ . Then  $E_{j_0}^*$  is a stable equilibrium, while for  $j \neq j_0$ ,  $E_j^*$  are saddle points.

### Appendix C. Analysis of the aggregated model with migration corridors

We determine non-negative equilibria and their stability.

#### C.1. Positive equilibria

With  $\eta = (\eta_1, \dots, \eta_s)$ , let us denote  $\gamma_j = q_j + \kappa_j \omega_j \beta$ ,  $\Delta_j = \delta_j \omega_j \beta$ , and  $\sigma(\eta) = \sum_{j=1}^s g_j \eta_j$ . Equilibria verify:

$$\eta_j \left( \alpha D_j g_j \frac{G}{\sigma(\eta) + G} - \gamma_j \right) + \Delta_j = 0 \quad \forall j \in \{1, \dots, s\} \quad (\text{C.1})$$

or

$$\eta_j = \frac{(\sigma(\eta) + G) \Delta_j}{(\sigma(\eta) + G) \gamma_j - \alpha D_j g_j G} \quad \forall j \in \{1, \dots, s\} \quad (\text{C.2})$$

If  $\eta$  is a positive equilibrium, then  $\sigma(\eta) > M = \max_{j=1, \dots, s} (\alpha D_j g_j / \gamma_j - 1) G$ , otherwise one of the coordinates of  $\eta$  will be negative according to Eq. (C.2). By summing Eq. (C.2), it also verifies

$$\sigma(\eta) = \sum_{j=1}^s g_j \frac{(\sigma(\eta) + G) \Delta_j}{(\sigma(\eta) + G) \gamma_j - \alpha D_j g_j G} \quad (\text{C.3})$$

which is equivalent to  $\Gamma(\sigma(\eta)) = 0$ , where  $\Gamma : ]M, +\infty[ \rightarrow \mathbb{R}$  is given by:

$$\Gamma(x) = \sum_{j=1}^s g_j \frac{(x + G) \Delta_j}{(x + G) \gamma_j - \alpha D_j g_j G} - x \quad (\text{C.4})$$

We have

$$\Gamma'(x) = \sum_{j=1}^s g_j \frac{((x + G) \gamma_j - \alpha D_j g_j G) \Delta_j - (x + G) \Delta_j \gamma_j}{((x + G) \gamma_j - \alpha D_j g_j G)^2} - 1 \quad (\text{C.5})$$

$$= - \sum_{j=1}^s g_j \frac{\alpha D_j g_j G \Delta_j}{((x + G) \gamma_j - \alpha D_j g_j G)^2} - 1 \quad (\text{C.6})$$

$$< 0 \quad (\text{C.7})$$

Since  $\lim_{x \rightarrow M^+} \Gamma(x) = +\infty$  and  $\lim_{x \rightarrow +\infty} \Gamma(x) = -\infty$ , there exists a unique solution of the equation  $\Gamma(x) = 0$ . We denote this solution as  $\sigma^*$ .

From (C.2), we now deduce the existence of a positive equilibrium  $\eta^*$  that verifies Eq. A.9 and which is uniquely defined by

$$\eta_j^* = \frac{(\sigma^* + G) \Delta_j}{(\sigma^* + G) \gamma_j - \alpha D_j g_j G} \quad \forall j \in \{1, \dots, s\} \quad (\text{C.8})$$

#### C.2. Stability of equilibrium $\eta^*$

We now determine the elements of the Jacobian: for all  $j \in \{1, \dots, s\}$ , we have

$$J_{j,j}^* = \alpha D_j g_j G \frac{\sum_{j'=1}^s g_{j'} \eta_{j'}^* + G - \eta_j^* g_j}{\left( \sum_{j'=1}^s g_{j'} \eta_{j'}^* + G \right)^2} - \gamma_j \quad (\text{C.9})$$

$$= - \frac{\Delta_j}{\eta_j^*} \frac{\alpha D_j g_j G \eta_j^* g_j}{\left( \sum_{j'=1}^s g_{j'} \eta_{j'}^* + G \right)^2} \quad (\text{C.10})$$

$$< 0 \quad (\text{C.11})$$

and for  $j \neq k$ ,

$$J_{j,k}^* = - \frac{\eta_j^* \alpha D_j G g_j g_k}{\left( \sum_{j'=1}^s g_{j'} \eta_{j'}^* + G \right)^2} \quad (\text{C.12})$$

$$< 0 \quad (\text{C.13})$$

Let us denote

$$\Delta = \text{diag} \left( \frac{\Delta_1}{\eta_1^*}, \dots, \frac{\Delta_s}{\eta_s^*} \right) \quad (\text{C.14})$$

$$A = \frac{\alpha G}{\left( \sum_{j=1}^s g_j \eta_j^* + G \right)^2} (D_1 g_1 \eta_1^*, \dots, D_s g_s \eta_s^*) \quad (\text{C.15})$$

$$H = (g_1, \dots, g_s) \quad (\text{C.16})$$

Vector  $A$  and  $H$  are positive and matrix  $\Delta$  has positive diagonal elements. We have  $J^* = -\Delta - A^T H$ . Let  $\lambda = a + ib$  be an eigenvalue of  $J^*$ . Because  $\bar{\lambda}$  is also an eigenvalue, we consider the case where  $b > 0$ . Let  $X$  be an eigenvector associated to  $\lambda$ .  $Y = (\overline{HX})X$  is also an eigenvector associated to  $\lambda$ . Let us write  $Y = U + iV$ , where  $U = (u_1, \dots, u_s)^T$  and  $V = (v_1, \dots, v_s)^T$ .  $HY = H(\overline{HX})X = HX(\overline{HX}) = |HX|^2$ , thus  $HY$  is real and non-negative, i.e.  $HU \geq 0$  and  $HV = 0$ .

$\lambda$  verifies  $-\Delta Y - A^T H Y = \lambda Y$ , and so the following equation holds:

$$-(\Delta + \lambda I)Y = (HY)A^T \quad (\text{C.17})$$

By separating real and imaginary parts, the equation is equivalent to

$$\begin{cases} -(\Delta + aI)U + bV = (HU)A^T \\ (\Delta + aI)V + bU = 0 \end{cases} \quad (\text{C.18})$$

Now we suppose that  $a \geq 0$ . The second equation from (C.18) implies that for  $j \in \{1, \dots, s\}$ ,  $v_j$  and  $u_j$  have opposite signs. Since  $HU = HY \geq 0$ , we deduce from the first equation that  $\forall j \in \{1, \dots, s\}$ ,

$$-(\Delta_{jj} + a)u_j + bv_j \geq 0 \quad (\text{C.19})$$

and so  $u_j \leq 0$  and  $v_j \geq 0$ . But this implies that  $HU \leq 0$ . So  $HU = 0$ , and so  $U = V = 0$ , which is impossible. That means that  $a < 0$ , and so  $Re(\lambda) < 0$ .

All the eigenvalues have a negative real part,  $\eta^*$  is a stable equilibrium.

## References

- Auger, P., Bravo de la Parra, R., Poggiale, J.-C., Sanchez, E., Sanz, L., 2008a. Aggregation methods in dynamical systems variables and applications in population and community dynamics. *Phys. Life Rev.* 5, 79–105.
- Auger, P., Bravo de la Parra, R., Poggiale, J.-C., Sanchez, E., Nguyen Huu, T., 2008b. Aggregation of variables and applications to population dynamics. In: Magal, P., Ruan, S. (Eds.), *Structured Population Models in Biology and Epidemiology*. Lecture Notes in Mathematics, vol. 1936, Mathematical Biosciences Subseries, Springer, Berlin, pp. 209–263.
- Auger P., Poggiale J.-C., Sanchez E., 2012. A review on spatial aggregation methods. *Ecol. Complex.* 10, 12–25.
- Auger, P., Roussarie, R., 1994. Complex ecological models with simple dynamics. From individuals to populations. *Acta Biotheor.* 42, 111–136.
- Auger, P., Poggiale, J.-C., 1995. Emerging properties in population dynamics with different time scales. *J. Biol. Syst.* 3 (2), 591–602.
- Blaxter, K.L., 1980. Working Party on Nutrient Requirements of Ruminants. Commonwealth Agricultural Bureaux for the Agriculture research Council.
- Carr, J., 1981. *Applications of Centre Manifold Theory*. Springer-Verlag, New York.
- El Abdllaoui, A., Auger, P., Kooi, B.W., Bravo de la Parra, R., Mchich, R., 2007. Effects of density-dependent migrations on stability of a two-patch predator-prey model. *Math. Biosci.* 210 (1), 335–354.
- Fancy, S.G., White, R.G., 1985. Incremental cost of activity. In: Hudson, R., White, R. (Eds.), *Bioenergetics of Wild Herbivores*. CRC Press, Boca Raton, FL, USA.
- Fenichel, N., 1971. Persistence and smoothness of invariant manifolds for flows. *Indiana Univ. Math. J.* 21 (3), 193–226.
- Hirsch, M.W., Pugh, C.C., Schub, M., 1970. Invariant manifolds. *Bull. Am. Nat.* 153, 1015–1019.
- Illius, A.W., Gordon, L.J., 1992. Modeling the nutritional ecology in ungulate herbivores: evolution of body size and competitive interactions. *Oecologia* 89, 428–434.
- Iwasa, Y., Andreasen, V., Levin, S., 1987. Aggregation in model ecosystems I. Perfect aggregation. *Ecol. Model.* 37, 287–302.
- Iwasa, Y., Levin, S., Andreasen, V., 1989. Aggregation in model ecosystems II. Approximate aggregation. *Math. Med. Biol.* 6, 1–23.
- Kshatriya, M., 1998. Spatial distribution of individuals based on ideal free distribution. PhD thesis, University of Miami.
- Ludwig, F., De Kroon, H., Prins, H.H., 2008. Impact of savanna trees on forage quality for large African herbivore. *Oecologia* 155, 487–496.
- Morozov, A., Sen, M., Banerjee, M., 2012. Top-down control in a patchy environment, Revisiting the stabilizing role of food-dependent predator dispersal. *Theor. Popul. Biol.* 81, 9–19.
- Murray, M.G., 1995. Specific nutrient requirement and migrations of wildebeest. In: Sinclair, A.R.E., Arcese, P. (Eds.), *Serengeti II: Dynamics, management and conservation of an ecosystem*. The university of Chicago Press Chicago, Ill, pp. 231–256.
- Western, D., Nightingale, D.L.M., 2004. Environmental change on the vulnerability of pastoralist to drought: The Maasai in Amboseli, Kenya, Africa Environment Outlook Case Studies, United Nations Environment Programme. Nairobi.
- Western, D., 1975. Water availability and its influence on the structure and dynamics of the savanna large mammal community. *E. Afr. Wildlife J.* 13, 265–286.